IEEE Access
Multidisciplinary | Rapid Review | Open Access Journal

Date of publication xxxx 00, 0000, date of current version xxxx 00, 0000.

Digital Object Identifier 10.1109/ACCESS.2017.Doi Number

A New Primary Protection Method with Received Power-based 3D Antenna Rotation Range Prediction for Dynamic Spectrum Access

Hiroto Kuriki[1], Keita Onose[1], Ryota Kimura[1], and Ryo Sawai[1]

[1] Sony Corporation, Shinagawa-ku, Tokyo, 141-8610 Japan

Corresponding author: Hiroto Kuriki (e-mail: Hiroto.Kuriki@sony.com).

This research is supported by the Ministry of Internal Affairs and Communications in Japan (JPJ000254).

ABSTRACT We propose a new primary protection method for Dynamic Spectrum Access (DSA), in which a secondary system uses a frequency band assigned to a primary system. Following a DSA implementation plan in Japan, we take care of a practical scenario where a primary system's transmission station (PTS) moves along a predefined course or area, and a corresponding primary reception station (PRS) keeps its antenna boresight facing towards the moving PTS. For accurate interference calculation from the secondary to the primary systems in this scenario, the proposed method takes the movement of the PTS into account and predicts a range of angle variation of the PRS's antenna boresight based on received signal powers from the PTS to the PRS. We conducted computer simulations in three different practical scenarios to demonstrate the effectiveness of the proposed method. The simulation results show that the proposed method can increase the number of available secondary base stations (SBSs) by up to 1.93 times compared to a conventional method.

INDEX TERMS 5G mobile communication, cognitive radio, dynamic spectrum access, field pickup unit (FPU), microwave link, spectrum sharing.

I. INTRODUCTION

As more user devices connect to the Internet worldwide, mobile communication traffic is growing exponentially [1]. To accommodate increasing traffic, 5G systems have been introduced around the world [2]. However, it is hard to allocate additional spectrums for the 5G systems because many of the frequency bands identified for International Mobile Telecommunications (IMT) have already been allocated to existing wireless systems [3]. To solve this problem and make more efficient use of spectrum resources, dynamic spectrum access (DSA) has been actively developed in some countries [4], [5]. DSA allows wireless systems (hereinafter, they are called secondary systems) to use of frequency resources unused in terms of time and/or space by existing wireless systems (hereinafter, they are called primary systems). In DSA, a spectrum management system (SMS) is introduced to control signal transmissions of the secondary systems and to make an interference level caused by the secondary systems lower than an allowable level for the primary system (hereinafter, this technology is called primary protection).

In Europe and the United States, the DSA systems have already been legislated and standardized, e.g., TV Band White Spaces (TVWS) in the UK and the United States, Licensed Shared Access (LSA) in the EU [6]–[11], and Citizens Broadband Radio System (CBRS) in the US [12][13]. CBRS has begun as an initial commercial deployment (ICD) phase for fourth-generation mobile communication (4G) systems since September 2019 [13]. Then, after the ICD phase, full-scale commercial deployment of CBRS has been operating successfully since January 2020 [14]. In CBRS, an SMS which is called as Spectrum Access System (SAS) controls availability of secondary 4G systems and transmission parameters such as operational frequency channels and transmission powers of radio stations of the secondary systems to protect federal radar systems, fixed wireless access, and fixed-satellite services as primary systems [15].

In Japan, some feasibility studies of DSA for commercial deployment also have begun to allocate frequency bands for the 4G/5G systems [16], [17]. The Ministry of Internal Affairs

and Communications announced that a commercial deployment of DSA with an SMS will launch in a 2.3 GHz band (Long-Term Evolution (LTE) Band 40 and New Radio (NR) Band n40) from 2021 [18]. In the 2.3 GHz band, microwave link systems, which is named as Field Pickup Unit (FPU), have already operated by broadcasters [19]. Therefore, FPU and 4G/5G systems become primary and secondary systems, respectively. FPU is composed of a pair of a primary transmission station (PTS) and a primary reception station (PRS). Fig. 1 illustrates an example of communications in FPU. It is mainly used for video content delivery of road races, e.g. marathon races, and then a PTS equipped with a camera and a vehicle sends images and videos to a PRS in one-way communications. The PRS is fixedly installed on buildings or mountains while the PTS moves on a predefined route of a road race. To achieve high quality video transmission between the fixed PRS and the moving PTS, a directional antenna boresight of the PRS is rotated for tracking the moving PTS manually by field workers [20]. This situation is very different from those of DSA in the other countries, where the antennas of the primary systems' radio stations do not rotate depending on the location of the primary systems' other radio stations in their operation. Therefore, conventional SMSs and their primary protection methods did not take care of the antenna rotations caused by the movement of other radio stations.

To use the frequency band assigned to FPU more efficiently, the SMS needs to take the rotations of the PRS's antenna boresight into account. However, it is hard to obtain information of the rotations from the FPU operators directly. Therefore, in this paper, we propose a new primary protection method with antenna rotation range prediction. In our proposed method, the SMS considers possible ranges of azimuth and elevation angles of the PRS's antenna boresight rotation in calculation of potential interferences from the SBSs to the PRS. The SMS predicts the ranges of the angles based on received powers from the PTS to the PRS. The received powers are estimated by a predetermined propagation model, the information of the PRS position and that of the predefined route where the PTS moves. Then the SMS uses the predicted ranges of the PTS's antenna rotation in the interference calculation. The predicted ranges help improve accuracy of the interference calculation and then increase availability of the secondary systems in DSA. In this paper we demonstrate effectiveness of our proposed method by computer simulations. In a previous paper, we preliminarily evaluated a primary protection method in a simple urban scenario [21]. On the other hand, in this paper, we consider various and more practical deployment scenarios such as urban, suburban, and rural areas in Japan. The simulation results show that our proposed method is superior to a conventional method and that the proposed method drastically increases the availability of the secondary system in all the scenarios.

The rest of this paper is organized as follows. An overview of DSA is briefly explained in Section II. Section III describes a conventional primary protection method which is adopted in CBRS. Section IV explains the new primary protection method and its procedure. In Section V, we discuss performance of the conventional and proposed methods in the three scenarios through the simulation results. Finally, remarks of this paper are concluded in Section VI.

II. OVERVIEW OF DSA ARCHITECTURE

Fig. 2 shows a structure of DSA which we discuss in this paper. A main component of DSA is the SMS (e.g., geo-location database (GLDB) in TVWS, LSA controller in LSA, and SAS in CBRS). The SMS connects with secondary systems' radio stations via public or private networks and acquires operational information of the secondary radio stations, e.g. location information, transmission powers, frequency channels and so on. The SMS also connects with an external database which is operated by e.g. government agencies. From the database, the SMS acquires operational information of primary systems' radio stations including installed positions, moving areas, transmission powers, and date and time of use of the primary systems. By using the acquired information, the SMS calculates potential interferences from the secondary systems to the primary systems. Then it determines transmission parameters of the secondary systems to make an aggregate interference from the secondary systems to the primary systems lower than an allowable level. The parameters include maximum acceptable transmission powers, frequency channels, and availability/suspension of radio stations in the secondary systems. Then the SMS commands

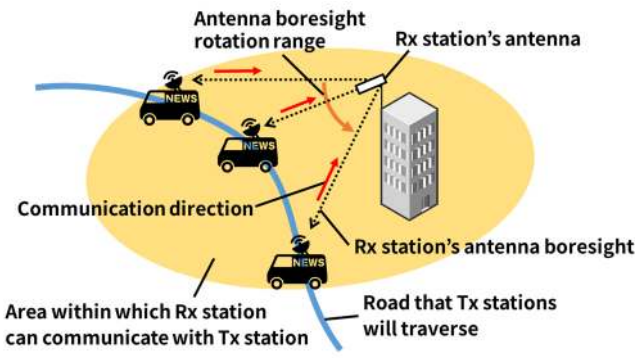

FIGURE 1. Communications between PRS and PTS in FPU.

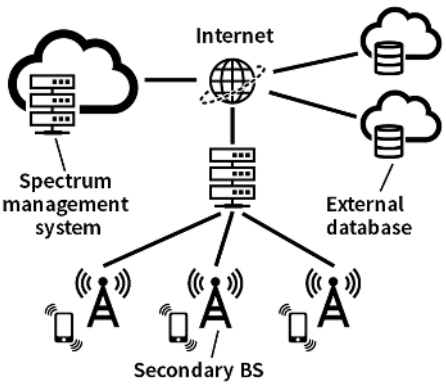

FIGURE 2. A structure of DSA.

the secondary systems' radio stations to change their transmission parameters immediately.

In this paper, the PRSs of the FPU and the SBSs of the 4G/5G systems are assumed to be as the primary and secondary systems' radio stations, respectively. To protect the PRS, the SMS allows or suspends a signal transmission of each SBS based on the availability. The SMS determines a list which contains SBSs to be suspended. Hereinafter, the list is called as an SBS suspension list (SBS-SL). In the followings, we explain how the SMS determines the SBS-SL in the conventional and proposed methods.

III. CONVENTIONAL PRIMARY PROTECTION

In this paper, we consider a primary protection method which is adopted to calculate the SBS-SL (which is called as the dynamic protection area move list) in CBRS as a conventional method [22]–[24]. Because the conventional method does not take care of the range of the PRS's antenna boresight rotation, the SMS determines the SBS-SL with assuming that the PRS's antenna boresight rotates 360 degrees in the horizontal plane and its vertical antenna pattern is omni-directional. Fig. 3 illustrates the calculation of the interference power from each SBS to the PRS deployed at a point R. The azimuth angle of the PRS's antenna boresight is represented as φ. In the conventional method, to ensure the protection of the PRS even when the limited range of variation of the PRS's antenna boresight direction is not provided, the SMS sets the range of φ to $0° \le \varphi < 360°$. Then the calculation of the SBS-SL must be performed individually for all φ within $0° \le \varphi < 360°$. However, if φ remains a continuous value, infinite number of calculations are required. Therefore, the azimuth angle is sampled at interval $\Delta\varphi$ within the range of $0° \le \varphi < 360°$. The sampled azimuth angles are expressed as $\varphi_i = 0, \Delta\varphi, 2\Delta\varphi, \dots, i\Delta\varphi, \dots, (N_s - 1)\Delta\varphi$, where N_s is the sampling number and $(N_s - 1)\Delta\varphi$ is less than 360 degrees.

After that, the SMS calculates a tentative SBS-SL for each φ_i, M_i, which is a SBS-SL assuming that the azimuth angle of the PRS's antenna boresight is set to φ_i. To calculate the tentative SBS-SL, the SMS forms a list $S = [BS_0, BS_2, \dots, BS_{N_{\mathrm{BS}}-1}]$, where N_{BS} is the total number of the SBSs in the list, and BS_j is the j-th SBS which interferes to the PRS. In the list S, the SBSs are sorted in ascending order of $P^{\varphi_i}_{BS_j \to R}$ $(0 \le j < N_{\mathrm{BS}})$, which is the interference power from the j-th SBS to the PRS when the azimuth angle of the PRS's antenna boresight is φ_i. As shown in Fig. 3, $P^{\varphi_i}_{BS_j \to R}$ can be expressed as follows:

$$P^{\varphi_i}_{BS_j \to R} = P_{BS_j} + G_{BS_j \to R} - L_{BS_j \to R} - L_{Rx} + G^{\varphi_i}_{R \to BS_j}, \quad (1)$$

where P_{BS_j} (dBm) is a conducted power of BS_j, and $G_{BS_j \to R}$ (dB) is an antenna gain of BS_j in the direction to the point R, $L_{BS_j \to R}$ (dB) is a propagation loss from BS_j to the PRS, L_{Rx} (dB) is a feeder loss of the PRS, $G^{\varphi_i}_{R \to BS_j}$ (dB) is an antenna gain of the PRS with the azimuth angle of the antenna boresight is φ_i in the direction to BS_j. In the conventional method, the SMS considers the antenna gains of both the SBS and the PRS in terms of the horizontal antenna patterns. After calculating $P^{\varphi_i}_{BS_j \to R}$, the SMS chooses the largest j_i which satisfies that the aggregate interference power $I_{aggregate,j_i}$ is less than or equal to an allowable interference power for the PRS $I_{allowed}$ (dBm). The condition of the aggregate interference $I_{aggregate,j_i}$ can be expressed as follows:

$$I_{aggregate,j_i} = \sum_{j=0}^{j_i} P^{\varphi_i}_{BS_j \to R} \le I_{allowed}. \quad (2)$$

Then the SBS-SL corresponding to φ_i is determined to be a set $M_i = \{BS_{j_i+1}, BS_{j_i+2}, \dots, BS_{N_{\mathrm{BS}}-1}\}$. Finally, the SMS obtain the SBS-SL corresponding to the PRS M by calculating the union of all M_i as follows:

$$M = \bigcup_{i=0}^{N_s-1} M_i. \quad (3)$$

Then the aggregate interference power from SBSs not include in M is less than or equal to $I_{allowed}$ for all φ_i.

IV. PROPOSED PRIMARY PROTECTION

Fig. 4 compares differences between the conventional and proposed method. Because the conventional method assumes 360 degrees of the range of the PRS's antenna boresight in the horizontal plane, it overestimates the potential aggregate interference from the SBSs to the PRS. For example, as shown in Fig. 4 (a), the potential aggregate interference may contain those from the SBSs which the PRS's antenna boresight does

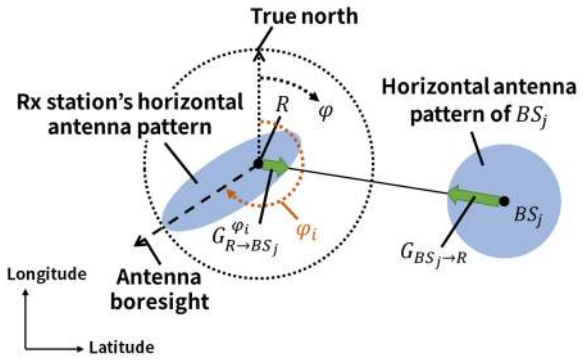

FIGURE 3. Calculation of received power from each SBS to PRS in conventional method. $\varphi = 0°$ points to the true north and that clockwise is a positive direction of φ.

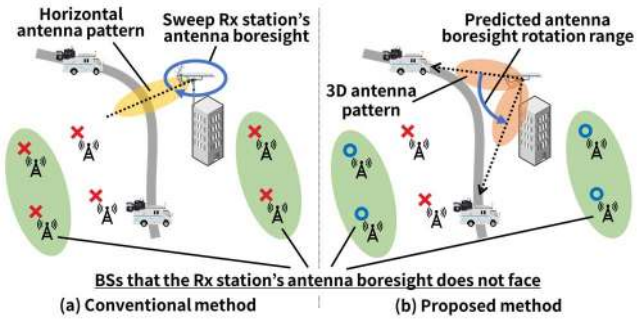

FIGURE 4. Conventional method versus proposed method. In the figure, circles mean available SBSs and crosses mean unavailable ones.

not face. As a result, the SMS may add these SBSs to the SBS-SL while these SBSs may cause less interferences to the PRS.

To solve this overestimation problem, our proposed primary protection method predicts the ranges of azimuth and elevation angles of the PRS's antenna boresight by estimating received powers from the PTS to the PRS. The received powers can be estimated based on the location of the fixed PRS and the trajectory of the PTS, that is, the predefined route of the race. Then the SMS calculates the aggregate interference by sweeping the PRS's antenna boresight within the predicted range. Therefore, the proposed method can calculate the aggregate interference more accurately and increase the availability of the SBSs which cause less interference to the PRS as shown in Fig. 4 (b).

A. ANTENNA ROTATION RANGE PREDICTION

In contrast to the conventional method, the proposed method is performed in two steps: antenna rotation range prediction and SBS-SL calculation. This and the following subsections describe details of the steps.

In the first step, the proposed method predicts the range of the PRS's antenna boresight rotation based on received power from the PTS to the PRS. Fig. 5 explains a positional relationship among the fixed PRS, the trajectory of the PTS and the range of the PRS's antenna boresight rotation. The location of the PRS and the trajectory where the PTS moves are represented as R and f, respectively. The elevation angle of the PRS's antenna boresight, θ_{φ}, and the point on f, T_{φ}, can be uniquely determined by the azimuth angle of the PRS's antenna boresight φ. To predict the range of the PRS's antenna boresight rotation, the SMS estimates the received power from the PTS located at T_{φ} to the PRS located at R. As mentioned in Section I and Fig. 1, it is assumed that the PRS's antenna boresight is directed to T_{φ} manually. The received power, $P_{T_{\varphi}\to R}$ (dBm), can be expressed as follows:

$$P_{T_{\varphi}\to R} = EIRP_{Tx} - L_{T_{\varphi}\to R} - L_{Rx} + G_{Rx}. \quad (4)$$

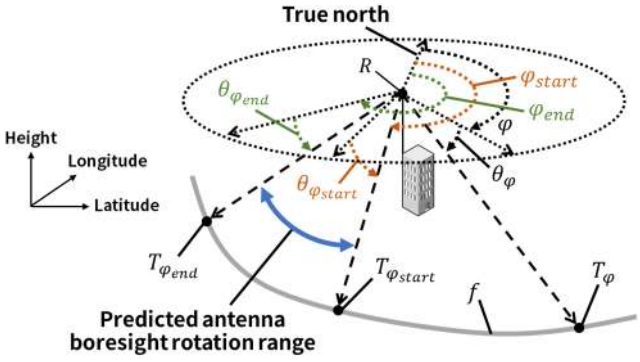

FIGURE 5. An overview of the PRS's antenna boresight rotation range prediction. The true north is defined by azimuth 0° and clockwise is a positive direction of the azimuth domain. Also, horizontal and nadir directions are set to elevation angle 0° and −90°, respectively.

$EIRP_{Tx}$ (dBm) is an EIRP (equivalent isotopically radiated power) of the PTS. $L_{T_{\varphi}\to R}$ (dB) is the propagation loss from T_{φ} to R. L_{Rx} (dB) and G_{Rx} (dB) are a feeder loss and an antenna gain of the PRS, respectively. Here, G_{Rx} is equal to the maximum antenna gain of the PRS because the PRS's antenna boresight is assumed to direct T_{φ}. The predicted antenna rotation range can be defined as a range of $\varphi_{start} \le \varphi \le \varphi_{end}$, where $P_{required}$ (dBm) is a required received power of FPU for stable video reception at the PRS, and φ_{start} and φ_{end} are the minimum and maximum azimuth angles which satisfy $P_{required} \le P_{T_{\varphi}\to R}$, respectively.

B. SECONDARY BS SUSPENSION LIST CALCULATION

As well as in the conventional method, the SMS samples the angles with replacing the range to $\varphi_{start} \le \varphi \le \varphi_{end}$. As a result, the sampled azimuth angles become $\varphi_i = \varphi_{start}, \varphi_{start} + \Delta\varphi, \dots, \varphi_{start} + i\Delta\varphi, \dots, \varphi_{start} + (N_s - 1)\Delta\varphi$. Then the SMS calculates the tentative SBS-SLs for all the sampled angles. $P^{\varphi_i}_{BS_j\to R}$ is calculated by using Eq. (1). As shown in Fig. 6, in the proposed method, the SMS uses the PRS's 3D antenna pattern based on φ_i and θ_{φ_i} for the antenna gains of the PRS $G^{\varphi_i}_{R\to BS_j}$ in Eq. (1). Also, it uses the 3D antenna pattern of BS_j for the antenna gains of the SBS $G_{BS_j\to R}$. After calculating $P^{\varphi_i}_{BS_j\to R}$, the SMS determines a set $M_i = \{BS_{j_i+1}, BS_{j_i+2}, \dots, BS_{N_{\mathrm{BS}}-1}\}$ for each φ_i by using the maximum index j_i which satisfies the condition Eq. (2). Finally, the SMS obtains the SBS-SL for the PRS M by using Eq. (3) as well as the conventional method.

V. EVALUATION BY SIMULATION

A. DEPLOYMENT SCENARIOS

We evaluated and compared the conventional and proposed methods by computer simulations under three scenarios. In each scenario, a PRS at a different location was protected from the SBSs. Blue dots in Fig. 7 represent the locations of the three PRSs. In the first scenario (S1), we assumed that a PRS with very high antenna height (400 m) was deployed in an urban area (Tokyo, Japan). In the second scenario (S2), a PRS with middle antenna height (50 m) was deployed in a suburban

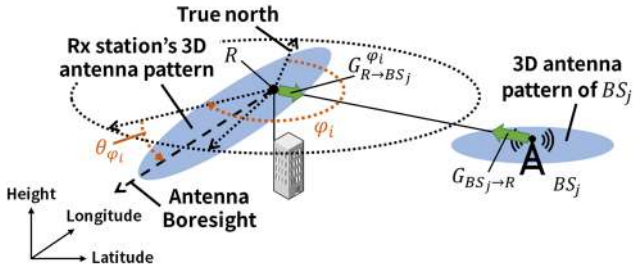

FIGURE 6. Calculation of received power from each SBS to PRS in proposed method.

This article has been accepted for publication in a future issue of this journal, but has not been fully edited. Content may change prior to final publication. Citation information: DOI 10.1109/ACCESS.2021.3081112, IEEE Access

area (Kanagawa, Japan). In the third scenario (S3), we assumed a PRS in a high-altitude rural area (Kanagawa, Japan), where the height above sea level was about 1300 m. A red line in Fig. 7 represents a route where the PTS moved along with in the three scenarios.

We assumed that the SBSs were deployed in Tokyo's 23 wards and densely inhabited districts (DIDs) [25], as illustrated in Figs. 8 and 9 respectively. In the Tokyo's 23 wards, intervals between the SBSs were set to 600 m in the latitude and longitude directions [26]. In the DIDs, the intervals were 1200 m.

FIGURE 7. Locations of three PRSs and a route of race where PTS of FPU is moved.

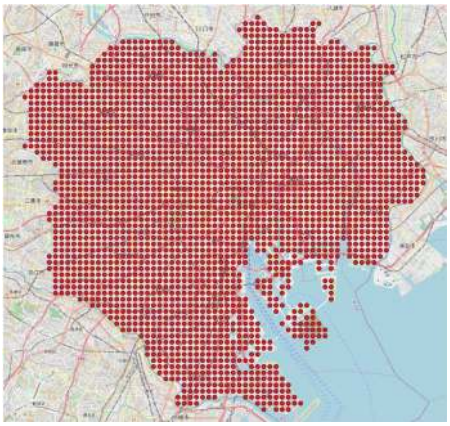

FIGURE 8. Locations of SBSs in Tokyo's 23 wards (red dots).

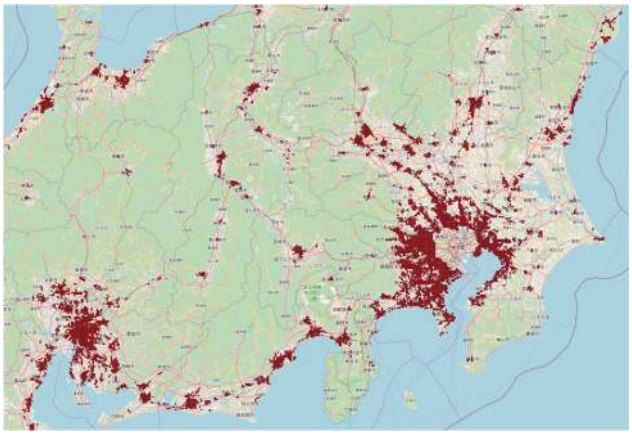

FIGURE 9. Locations of SBSs in DIDs (red dots).

B. SIMULATION PARAMETERS

Table I shows the conditions of the clear-air method of ITU-R P.452-16 used as a propagation model in the simulations [27], [28]. The propagation loss is calculated based on the actual topography.

Tables II and III show radio parameters of the FPU [28]–[30] and those of the SBSs [30], [31], respectively. We

TABLE I
CONDITIONS FOR CLEAR-AIR METHOD IN ITR-R P.452 [27]

Parameters	Value
Required time percentage for which the calculated propagation loss is not exceeded	20 % between the PRS and SBSs [28], 0.001% between the PTS and PRS
Polarization	Vertical
Clutter category	S1: Dense urban, S2: Dense suburban, S3: Village centre
Dry air pressure [hPa]	1013
Air Temperature [degree]	28

TABLE II
PRIMARY FPU RADIO PARAMETERS [29]

Parameters		Value
Carrier Frequency [GHz]		2.35
Bandwidth [MHz]		17.2
Tx	Tx Power [dBm]	46.0
	Antenna Gain [dBi]	5.2
	Horizontal Antenna Pattern	Omni-directional
	Vertical Antenna Pattern	Directional [30] (HPBW: 23 degrees, Maximum attenuation: 30 dB)
	Antenna Height [m]	3.5
	Feeder Loss [dB]	1.5
Rx	Antenna Gain [dBi]	14.0
	Horizontal/Vertical Antenna Pattern	Directional [30] (HPBW: 30 degrees, Maximum attenuation: 30 dB)
	Antenna Height [m]	S1: 400, S2: 50, S3: 5
	Feeder Loss [dB]	1.5
	Noise Figure [dB]	4.0
	Required Received Power ($P_{required}$) [dBm]	−81.4
	Allowable I/N [dB]	−10.0 [28]
	Allowable Interference Power ($I_{allowed}$) [dBm]	−107.4

TABLE III
SECONDARY BASE STATION PARAMETERS [30]

Parameters	Value
Carrier Frequency [GHz]	2.35
Bandwidth [MHz]	18.0
Tx Power [dBm/MHz]	20.0
Antenna Gain [dBi]	5.0
Horizontal Antenna Pattern	Omni-directional
Vertical Antenna Pattern	Directional [31]
Antenna Height [m]	10.0
Feeder Loss [dB]	0.0

This article has been accepted for publication in a future issue of this journal, but has not been fully edited. Content may change prior to final publication. Citation information: DOI 10.1109/ACCESS.2021.3081112, IEEE Access

assumed LTE (Long-term evolution)-Advanced for the SBSs and followed the parameters of small cell BSs described in [30].

C. EVALUATION RESULTS

In this subsection, SBSs within a line-of-sight (LOS) distance from the PRS, i.e., maximum distance between the PRS and SBS for LOS propagation [32], are considered in the SBS-SL calculations of both the conventional and proposed methods because these SBSs may cause strong impacts on the aggregate interferences. The LOS distance D (km) between two radio stations can be calculated as follows:

$$D = 4.12 \times \left(\sqrt{h_1} + \sqrt{h_2}\right), \quad (5)$$

where h_1 (m) and h_2 (m) are antenna heights above sea level of two radio stations' antenna. Eq. (5) implies that the LOS distance from the PRS and the numbers of SBSs within the LOS distance increases as the PRS's antenna height above sea level rises. Green dots in Figs. 10 (a), (b) and (c) represent the SBSs within the LOS distance on a map of the simulated areas in S1, S2 and S3, respectively. 6355, 4088 and 6975 SBSs were considered for the SBS-SL calculation in S1, S2, and S3, respectively. Yellow dots in Fig. 10 represent the SBSs beyond the LOS distance, which are absolutely excluded from the SBS-SL calculation and available in the secondary use manner due to large propagation losses by non-LOS (NLOS) conditions.

Figs. 11 (a) and (b) show the results of the SBS-SL calculated by the conventional and proposed methods in S1, respectively. The blue dots are the SBSs that are available, that is, the aggregate interference from these SBSs to the PRS is below the allowable level, even when the FPU is operating in the same frequency band simultaneously. The red dots are the SBSs that are unavailable when the FPU is used, that is, the SBSs that cause harmful aggregate interference to the PRS. In S1, the SBSs deployed in Tokyo's 23 wards are not available, regardless of the conventional or proposed method. On the other hand, the number of available SBSs deployed outside the 23 wards is increased by the proposed method. The conventional method can make 375 out of 6355 SBSs available. In contrast, the proposed method can make 622 out of 6355 SBSs available and increases the number of available SBSs within the LOS distance by 1.66 times compared to the conventional method.

Figs. 12 (a) and (b) show the results of the SBS-SLs calculated by the conventional and proposed methods in S2, respectively. The conventional method can make 259 out of 4088 SBSs available, and the proposed method can make 501 out of 4088 SBSs available. The proposed method can increase the number of available SBSs within LOS distance by about 1.93 times compared to the conventional method. In S2, the PRS's antenna boresight is mainly pointed in a northwestward direction because the PRS's coverage on the PTS's route in Fig. 7 is located at the northwest side of the PRS. The proposed method can predict this antenna rotation by calculating the PRS's coverage based on the received power and make some SBSs on the east side of the PRS available. Note that most of the SBSs within the LOS distance cause severe interference to the PRS in S2 because the LOS distance is shorter than those of the other scenarios. As a result, the number of available SBSs within LOS distance is small compared to the other scenarios, regardless of the conventional or proposed method.

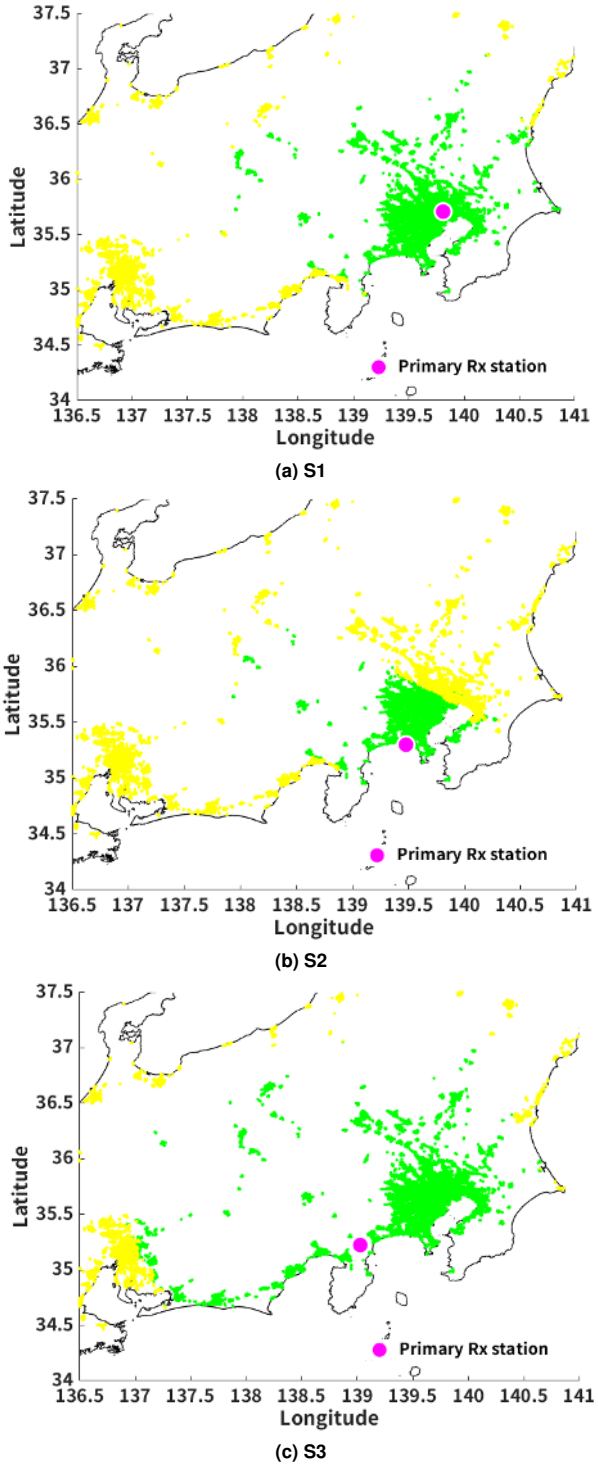

FIGURE 10. SBSs within LOS distance (green) and those beyond LOS distance (yellow) from PRS.

This article has been accepted for publication in a future issue of this journal, but has not been fully edited. Content may change prior to final publication. Citation information: DOI 10.1109/ACCESS.2021.3081112, IEEE Access

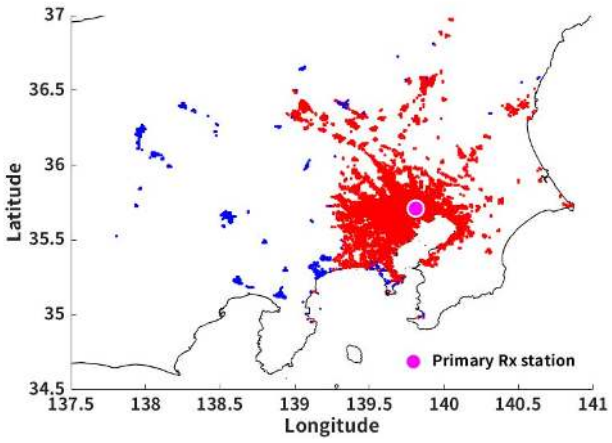

(a) Conventional method

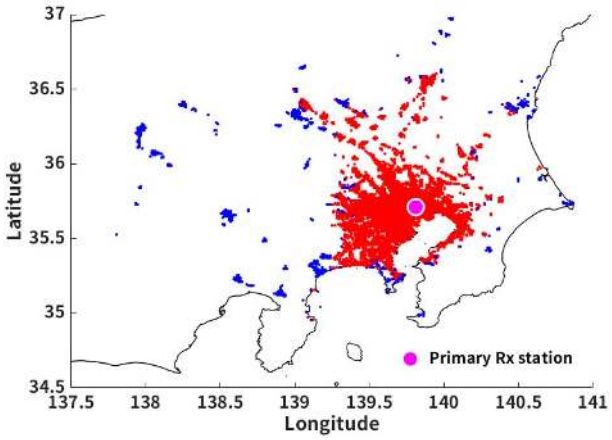

(b) Proposed method

FIGURE 11. Available and unavailable SBSs in S1.

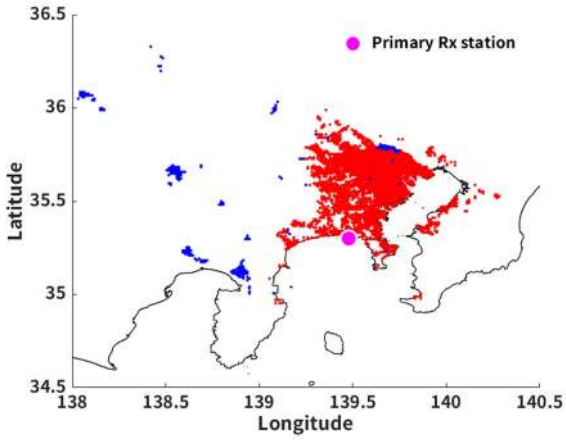

(a) Conventional method

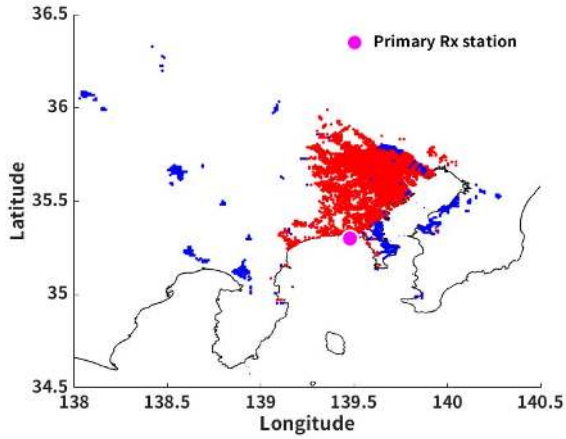

(b) Proposed method

FIGURE 12. Available and unavailable SBSs in S2.

Figs. 13 (a) and (b) show the results of the SBS-SLs calculated by the conventional and proposed methods in S3, respectively. The conventional method can make 1805 out of 6975 SBSs available, respectively whereas the proposed method can make 2316 out of 6975 SBSs available. The proposed method can increase the number of available SBSs within LOS distance by about 1.28 times compared to the conventional method in S3. These results show that some SBSs on the west and north side of the PRS become available by the proposed method. In S3, the PRS's antenna boresight is mainly pointed in an eastward direction because the PTS's route is located at the east side of the PRS, as illustrated in Fig. 7. By predicting this antenna rotation, the proposed method can improve the number of the available SBSs. Note that the LOS distance from the PRS is longer than those of the other scenarios in S3. Therefore, compared to the other scenarios, only a relatively small percentage of the SBSs within the LOS distance causes harmful interference to the PRS. As a result, compared to the other scenarios, relatively more SBSs within the LOS distance become available in S3 even by the conventional method. Conversely, there is little room for improvement by the proposed method in S3.

VI. CONCLUSION

We have proposed a new primary protection method with received power-based antenna rotation range prediction to increase the availability of the secondary 4G/5G systems under the secondary use manner. The proposed method does not require the primary system operator to provide the information of the PRS's antenna rotation ranges to the SMS. Instead, the proposed method predicts the ranges of azimuth and elevation angles of the PRS's antenna boresight based on the received powers from the PTS to the PRS, and then calculates the interferences from the SBSs to the PRS by sweeping the PRS's antenna boresight within the predicted ranges and using the 3D antenna pattern. Assuming the practical deployment of DSA in the 2.3 GHz band in Japan, we evaluated the proposed method in the three different scenarios, i.e. urban, suburban, and rural, by the computer simulations. The simulation results show that the proposed method increases the number of available SBSs within LOS

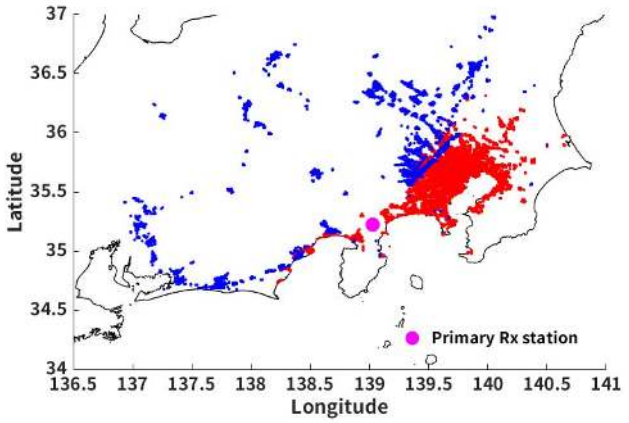

(a) Conventional method

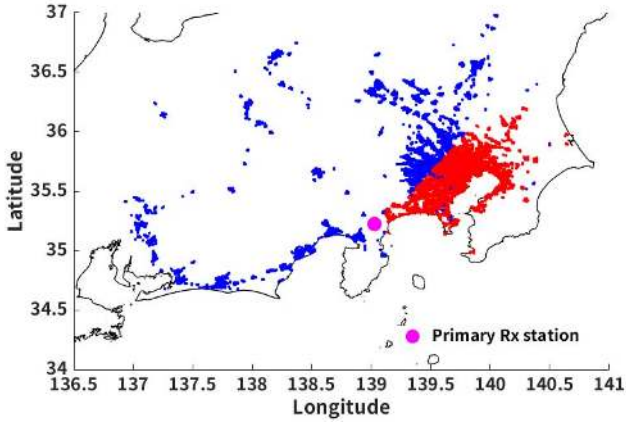

(b) Proposed method

FIGURE 13. Available and unavailable SBSs in S3.

distance by 1.66, 1.93 and 1.28 times compared to the conventional method in the scenarios respectively. These results indicate that the proposed method can allocate the 2.3 GHz band to the 4G/5G systems under the secondary use manner and that it is promising to solve the problem of frequency resource shortage.

REFERENCES

[1] "Cisco Annual Internet Report (2018–2023)," Cisco. San Jose, California, United States. Mar. 9, 2020. [Online]. Available: https://www.cisco.com/c/en/us/solutions/collateral/executive-perspectives/annual-internet-report/white-paper-c11-741490.pdf, Accessed on: May 10, 2021

[2] *IMT Vision - Framework and overall objectives of the future development of IMT for 2020 and beyond*, ITU-R Recommendation M.2083-0, Sep. 2015.

[3] "5G Spectrum GSMA Public Policy Position," GSMA Association. London, United Kingdom. Mar. 2020. [Online]. Available: https://www.gsma.com/spectrum/wp-content/uploads/2020/03/5G-Spectrum-Positions.pdf, Accessed on: May 10, 2021

[4] "Spectrum Sharing GSMA Public Policy Position," GSMA Association. London, United Kingdom. Jul. 2019. [Online]. Available: https://www.gsma.com/spectrum/wp-content/uploads/2019/09/Spectrum-Sharing-PPP.pdf, Accessed on: May 10, 2021

[5] M. D. Mueck, S. Srikantesware, and B. Badic, "Spectrum Sharing: Licensed Shard Access (LSA) and Spectrum Access System (SAS)," Intel. Santa Clara, California, United States. Version v1.0, Oct. 2015. [Online]. Available: https://www.intel.com/content/dam/www/public/us/en/documents/white-papers/spectrum-sharing-lsa-sas-paper.pdf, Accessed on: May 10, 2021

[6] "Unlicensed Operation in the TV Broadcast Bands; Additional Spectrum for Unlicensed Devices Below 900 MHz and in the 3 GHz Band," Federal Communications Commission (FCC). Washington, DC, United States. May 2004. [Online]. Available: https://docs.fcc.gov/public/attachments/FCC-04-113A1.pdf, Accessed on: May 10, 2021

[7] "Implementing TV White Spaces,". The Office of Communications (Ofcom). London, United Kingdom. Feb. 2015. [Online]. Available: https://www.ofcom.org.uk/__data/assets/pdf_file/0034/68668/tvws-statement.pdf, Accessed on: May 10, 2021

[8] "ECC Report 205 Licensed Shared Access (LSA)," European Conference of Postal and Telecommunications Administrations (CEPT). Copenhagen, Denmark. Feb. 2014. [Online]. Available: http://spectrum.welter.fr/international/cept/ecc-reports/ecc-report-205-LSA-2300-MHz-2400-MHz.pdf, Accessed on: May 10, 2021

[9] *Electromagnetic compatibility and Radio spectrum Matters (ERM); System Reference document (SRdoc); Mobile broadband services in the 2 300 MHz - 2 400 MHz frequency band under Licensed Shared Access regime*, ETSI TR 103 113 V1.1.1, Jul. 2013.

[10] D. Guiducci et al., "Sharing under licensed shared access in a live LTE network in the 2.3–2.4 GHz band end-to-end architecture and compliance results," in *Proc. 2017 IEEE Int. Symp. on Dynamic Spectrum Access Networks (DySPAN)*, USA, Mar. 2017, pp. 1–10.

[11] "Amendment of the Commission's Rules with Regard to Commercial Operations in the 3550-3650 MHz Band," Federal Communications Commission (FCC). Washington, DC, United States. Apr. 2014. [Online]. Available: https://docs.fcc.gov/public/attachments/FCC-14-49A1.pdf, Accessed on: May 10, 2021

[12] M. M. Sohul, M. Yao, T. Yang and J. H. Reed, "Spectrum access system for the citizen broadband radio service," in IEEE Communications Magazine, vol. 53, no. 7, pp. 18–25, Jul. 2015.

[13] "Wireless Telecommunications Bureau and Office of Engineering and Technology Approve Five Spectrum Access System Administrators to Begin Initial Commercial Deployments in the 3.5 GHz Band," Federal Communications Commission (FCC). Washington, DC, United States. Sep. 2019.

[14] "Wireless Telecommunications Bureau and Office of Engineering and Technology Approve Four Spectrum Access System Administrators for Full Scale Commercial Deployment in the 3.5 GHz Band and Emphasize Licensee Compliance Obligations in the 3650-3700 MHz Band under Part 96," Federal Communications Commission (FCC). Washington, DC, United States. Jan. 2020.

[15] *Signaling Protocols and Procedures for Citizens Broadband Radio Service (CBRS): Spectrum Access System (SAS) - Citizens Broadband Radio Service Device (CBSD) Interface Technical Specification*, WINNF-TS-0016 Version V1.2.4, Jun. 2019.

[16] Y. Hirano, "Social Implementation for the Dynamic Spectrum Access in Japan," in *Proc. 2020 IEICE General Conf*, Japan, Mar. 2020, BI-9-3. (in Japanese)

[17] Y. Kishi, H. Shinbo and T. Hayashi, "Research & Development to realize the advanced dynamic spectrum sharing system between different radio services," in *Proc. 2020 IEICE Society Conf*, Japan, Sep. 2020, BP-2-1. (in Japanese)

[18] "Frequency Reorganization Action Plan (FY2020 Second Revision)," Ministry of Internal Affairs and Communications (MIC). Tokyo, Japan. Nov. 2020. [Online] Available: https://www.soumu.go.jp/main_content/000704672.pdf (in Japanese)

[19] *1.2GHz / 2.3GHz-Band Portable OFDM Digital Transmission System for Television Program Contribution*, ARIB STD-B57 Version 2.2, Dec. 2013. (in Japanese)

[20] "Technical Requirements for Upgrading of Field Pickup Units," Ministry of Internal Affairs and Communications (MIC). Tokyo, Japan. Jun. 2013. [Online]. Available: https://www.soumu.go.jp/main_content/000287081.pdf (in Japanese), Accessed on: May 10, 2021

[21] H. Kuriki, K. Onose, R. Kimura and R. Sawai, "Primary Protection with Antenna Rotation Prediction for Dynamic Spectrum Access," in *Proc. the 23rd International Symposium on Wireless Personal Multimedia Communications (WPMC2020)*, Oct. 2020, pp. 163–168.

[22] *Requirements for Commercial Operation in the U.S. 3550-3700 MHz Citizens Broadband Radio Service Band*, WINNF-TS-0112 Version V1.9.0, Dec. 2019.
[23] SAS Testing and Interoperability Repository. [Online]. Available: https://github.com/Wireless-Innovation-Forum/Spectrum-Access-System, Accessed on: May 10, 2021
[24] M. Souryal, T. Nguyen and N. LaSorte, "3.5 GHz Federal Incumbent Protection Algorithms," in *Proc. 2018 IEEE International Symposium on Dynamic Spectrum Access Networks (DySPAN)*, Oct. 2018, pp. 1–5.
[25] "National land numerical information," Ministry of Land, Infrastructure, Transport and Tourism (MLIT). Tokyo, Japan. [Online]. Available: https://nlftp.mlit.go.jp/ksj/gml/datalist/KsjTmplt-A16-v2_3.html, Accessed on: May 10, 2021
[26] *Characteristics of terrestrial IMT-Advanced systems for frequency sharing/interference analyses*, ITU-R Recommendation M.2292-0, Dec. 2013.
[27] *Prediction procedure for the evaluation of interference between stations on the surface of the Earth at frequencies above about 0.1 GHz*, ITU-R Recommendation P.452-16, Jul. 2015.
[28] *System parameters and considerations in the development of criteria for sharing or compatibility between digital fixed wireless systems in the fixed service and systems in other services and other sources of interference*, ITU-R Recommendation F.758-7, Nov. 2019.
[29] "Technical Requirements for FPUs Using 1.2 GHz and 2.3 GHz bands for Ultra-high-definition Television Broadcasting System," Ministry of Internal Affairs and Communications (MIC). Tokyo, Japan. Jun. 2019. [Online]. Available: https://www.soumu.go.jp/main_content/000627910.pdf (in Japanese), Accessed on: May 10, 2021
[30] *Evolved Universal Terrestrial Radio Access (E-UTRA); Further advancements for E-UTRA physical layer aspects*, 3GPP TR 36.814 V9.2.0, Mar. 2017.
[31] *Reference radiation patterns of omnidirectional, sectoral and other antennas for the fixed and mobile service for use in sharing studies in the frequency range from 400 MHz to about 70 GHz*, ITU-R Recommendation F.1336-5, Jan. 2019.
[32] United States. Navy. Weather Research, *Meteorological Aspects of Radio-radar Propagation*. Belmont, VA, USA: U.S. Government Printing Office, 1960, pp. 15–61.

HIROTO KURIKI received the B.E. degree from Kyoto University, Kyoto, Japan, in 2016 and the Master of Informatics degree from Kyoto University, Kyoto, Japan, in 2018.

Since 2018, he has been a research engineer with R&D Center, Sony Corporation, Japan. He has authored several peer-reviewed international conference articles. His research interest includes the radio access network, core network, spectrum sharing, and private network.

He was a co-recipient of the Best Paper Award from ICETC 2020.

KEITA ONOSE received the B.E. and M.E. degrees in engineering from the University of Electro-Communications, Tokyo, Japan, in 2017 and 2019.

In 2019, he joined Sony Corporation and is currently a research engineer at R&D Center. His research interest includes cognitive radio, dynamic spectrum access, and radio propagation.

He was a co-recipient of the Best Paper Award from ICETC 2020.

RYOTA KIMURA earned his B.E. and M.E. degrees from Chuo University, Tokyo, Japan, in 2003 and 2005, respectively, and earned his Ph.D. degree from Waseda University, Tokyo, Japan, in 2008.

From 2002 to 2008, he was a trainee at National Institute of Information and Communications Technology, Kanagawa, Japan. From 2006 to 2008, he was also a research fellow of Japan Society for the Promotion of Science. In 2008, he joined Sony Corporation and is currently a senior manager at R&D Center. His research interests include cognitive radio, dynamic spectrum access, spectrum sharing, wireless LAN and 5G/beyond-5G cellular systems.

He was a co-recipient of the Best Paper Award from ICETC 2020.

RYO SAWAI received the B.E., M.E. and Ph.D. degrees in electrical and electronic engineering from Chuo University, Tokyo, Japan, in 1998, 2000 and 2002, respectively.

He is currently a deputy general manager at R&D Center, Sony corporation, Japan. He finished an executive Management of Technology (MOT) course at CICOM-ISL (Innovation Strategy and Leadership basic program) in 2013. His research interests include 4G/ 5G cellular technologies, advanced coding design, e.g. Turbo code/decoder and Low-Density Parity Check code/decoder, reconfigurable hardware architecture design, multi-antenna processing technologies, cognitive radio, multi/many core based processing technology and cloud architecture design.

He received IEEE VTS Japan Researcher's Encouragement Award in 2001. He was a co-recipient of the Best Paper Award from ICETC 2020.